RESISTIVE ARTIFACTS IN LIQUID-ION EXCHANGER MICROELECTRODE ESTIMATES OF Na^+ ACTIVITY IN EPITHELIAL CELLS

S. A. LEWIS AND N. K. WILLS, *Department of Physiology, Yale University School of Medicine, New Haven, Connecticut 06510 U.S.A.*

ABSTRACT In experiments on the rabbit urinary bladder epithelium we have identified an electrical artifact in certain liquid ion-sensitive microelectrodes. This artifact arises from the high electrical resistance of the ion-sensitive resins which in some cases are comparable to the resistance of the microelectrode glass wall. For Na^+-sensitive microelectrodes this situation led to shunting of the exchanger potential and consequently artifactually high calculations of intracellular Na^+ in the rabbit urinary bladder epithelium. A method for minimizing this shunting effect is described. After reduction of the shunt the frequency response of the Na^+-sensitive microelectrode was increased and the estimated a_i Na^+ was decreased to 7 mM.

INTRODUCTION

Liquid ion exchange resins have recently enjoyed widespread usage as a method for measuring intracellular ion activity, since these resins can be incorporated into relatively small microelectrode tips and still demonstrate a reasonable ion specificity. Three of the most common exchangers are: (*a*) a K^+ exchanger (Corning) which shows a selectivity of 50:1 over Na^+ when placed in an appropriately treated micropipette, (*b*) a Cl^- exchanger (Corning and Orion), and most recently (*c*) a Na^+ ligand which demonstrates a selectivity 20:1 over K^+ when incorporated into a micropipette (O'Doherty et al., 1979, and Steiner et al., 1979).

In contrast to conventional 3 M KCl microelectrodes, the ion-specific microelectrodes have very high electrical resistances ($>10^9$ Ω) and consequently a high input impedance amplifier (e.g., $>10^{15}$ Ω) must be used to reduce attenuation of the electrical signal. In this communication we report that signal attenuation can occur by electrical leakage through the glass wall of the microelectrode. Specifically we show that the Na^+ exchanger has an electrical resistance near or at the tip of the microelectrode which is comparable to that of the microelectrode glass wall. The resulting signal attenuation results in an overestimate of intracellular Na^+ activity in the rabbit urinary bladder epithelium. We offer a possible method to reduce or eliminate this artifact.

MATERIALS AND METHODS

Urinary bladders were obtained from adult male New Zealand white rabbits. The tissue was dissected, mounted, and placed between modified Ussing chambers (15 ml/chamber) designed to eliminate edge damage and to reduce hydrostatic gradients during microelectrode impalements (Lewis, 1977; Lewis et al., 1977).

Electrical Measurements

Transepithelial voltage (V_t) was monitored with two Ag-AgCl wires placed 10 mm apart and on opposite sides of the tissue and referenced to the serosal solution. Ag-AgCl electrodes placed at the end of each chamber were used to apply a transepithelial current (ΔI) to determine short circuit current (I_{sc}) and the transepithelial capacitance (C_t) (see Lewis and Diamond, 1976). All electrodes led to an automatic voltage clamp. V_t, I_{sc}, and microelectrode potentials (basolateral membrane potential V_{bl} and ion specific electrode potential V_i: V_{Na} (sodium) or V_K (potassium) were displayed on three digital voltmeters (Newport) interfaced to a Newport digital printer. The printer was triggered by an Anapulse stimulator (W-P Instruments Inc., New Haven, Conn.) to print V_t, I (current), and V_{bl} (basolateral potential measured from cell interior referenced to the serosal solution) during and after an applied current pulse (ΔI). The lapsed time between measuring the voltage deflections and the base line values was 750 ms. This system allowed an accurate monitoring of spontaneous V_t and V_{bl}, G_t (transepithelial conductance calculated as $\Delta I/\Delta V_t$), α (resistance ratio; see Lewis et al., 1977), and in some instances V_i (potential recorded by the ion-specific microelectrode from cell interior referenced to the serosal solution). In addition to measuring V_t, I_{sc}, V_{bl}, and V_i with the digital meters, these parameters were also displayed on a two channel strip chart recorder (Houston Instruments Div., Bausch & Lomb, Inc., Austin, Texas) and a four channel storage oscilloscope (Tektronix Inc., Beaverton, Ore.)

Microelectrodes

Corning redrawn pyrex glass tubing (#7740) with an o.d. of 1.2 mm and i.d. of 0.9 mm was used as stock for microelectrode fabrication.

Glass microelectrodes were pulled to tip diameters of <1 μm on a Narishige horizontal puller (resistance of 3 M KCl electrode = 20–40 MΩ). The tips of the pulled microelectrodes were dipped in a 2.5% (vol/vol) solution of tri-*n*-butylchlorosilane and 1 chloro-Napthalene, and then heat dried for 10 min. Na^+ exchanger was introduced through the tip to a column height of 100–300 μm. The microelectrode was then backfilled with 0.5 M NaCl. The microelectrode was placed in a Ag-AgCl half cell, mounted in a hydraulic microdrive unit, and then connected to the input of a high input impedence dual differential amplifier (WP Instruments, Model F223A). The microelectrode and amplifier were electrically isolated from the microdrive and the microdrive was isolated from ground. Na^+-sensitive microelectrodes were calibrated in 10^{-1}, 10^{-2}, and 10^{-3} M NaCl solutions. Selectivity to K^+ was determined by either 10^{-1} M KCl solution or mixed NaCl-KCl solutions. The Na^+-K^+ selectivity ratio of the Na^+ microelectrode was calculated using the Nicolsky equation (Eaton et al., 1975). K^+-sensitive microelectrodes were constructed and calibrated as previously described (Lewis et al., 1978). Conventional microelectrodes were connected via a Ag-AgCl half cell to the input of a differential electrometer (Model 750, WP Instruments).

Basolateral membrane potential was measured immediately before and after the use of the single barreled Na^+ and K^+ microelectrodes. Resistance ratios ($\alpha \equiv R_a/R_{bl}$, resistance ratio of apical to basolateral membrane) were measured for conventional, Na^+ and K^+ microelectrodes.

After measuring the potential difference between cell interior and serosal solution with the Na^+- and K^+-specific microelectrodes and conventional microelectrode, intracellular Na^+ and K^+ activities (a_i Na^+ and a_i K^+) were calculated using the Nicolsky equation (Eaton et al. 1975).

Solutions

The composition in mM of the bathing solution (NaCl Ringer's) was 111.2 NaCl, 25 $NaHCO_3$, 5.8 KCl, 2 $CaCl_2$, 1.2 $MgSO_4$, 1.2 KH_2PO_4, and 11.1 glucose. This solution was gassed with 95% O_2–5% CO_2 and maintained at a pH of 7.4 and a temperature of 37°C.

RESULTS

Intracellular Na^+ Activities

Single barrel Na^+- and K^+-selective microelectrodes were used to measure a_i Na^+ and a_i K^+ of the most apical cell layer of the rabbit urinary bladder. The mean a_i K^+ was 89 ± 9 mM

and was not statistically larger than our earlier measurement (Lewis et al., 1978). The mean a_i Na^+ (corrected for a_i K^+) was 19.0 ± 2.5 mM (n = 54). Fig. 1 shows marked variations in a_i Na^+. The mean measured resistance ratio (α_i) for the Na^+ specific microelectrodes was 4 (indicating for that cell that the apical membrane resistance is four times that of the basolateral membrane resistance), while the resistance ratio measured using the conventional microelectrodes (α) was 15 (i.e., apical membrane resistance is 15 times greater than the basolateral membrane resistance).

Artifacts

Although many hypotheses can be formulated to account for the variable a_i Na^+, most can be eliminated because of a lack of predicted effect on the voltage divider ratio. Four possibilities could account for such a large variability in a_i Na^+ and the difference in the voltage divider ratio as follows: (*a*) Individual cells might contain a variable (a_i Na^+) or similarly the cell population might be heterogeneous. (*b*) The ion exchanger by some effect may poison the cell, thus causing membrane resistance changes and Na^+ accumulation. (*c*) The Na^+-specific microelectrodes may not completely seal in the cell, i.e., impalement damage may cause a significant leak of ions into the cell interior as well as decrease the apparent apical resistance (Fig. 2 *a*). (*d*) The resistance of the ion exchanger at the tip of the microelectrode is comparable in magnitude to the resistance of the glass wall of the microelectrode. Therefore, this matching of impedances could cause an attenuation of both membrane potential and activity signal (Fig. 2 *b*).

In the present study and as previously found by Lewis et al. (1978), conventional microelectrodes did not measure a variable cellular potential that might be expected from a heterogenous population of cells. As for the second hypothesis, one might expect poisoning of the cell to be a time-dependent phenomenon, i.e., α_i should decrease and a_i Na^+ increase after impalement. This was not observed. As for the third explanation, cell disruption, Lewis et al. (1978) also explored the possibility of impalement damage. Their analysis was intended to identify damage in epithelial tissue; briefly, these authors showed that by taking the difference between the inverse resistance ratios measured with the ion specific microelectrode and a conventional (3 M KCl) microelectrode, one could obtain a ratio of apical membrane damage

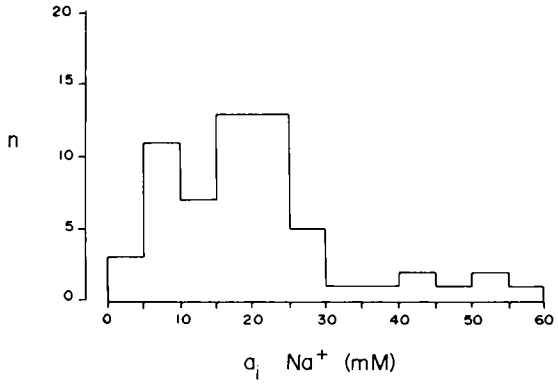

FIGURE 1 Histogram of measured intracellular sodium activity (a_i Na^+) in millimolar using sodium selective microelectrodes fabricated as described in Methods.

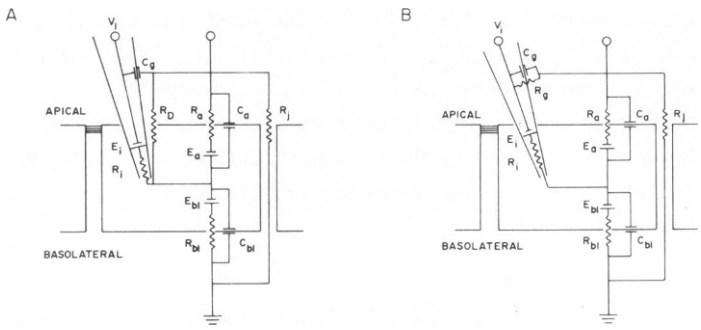

FIGURE 2 Illustration of two hypotheses for the lower resistance ratio (α_i) measured with Na^+-specific microelectrode. (*A*) Impalement damage or cell membrane disruption caused by the microelectrode entering the cell across the apical membrane. R_D is the damage resistance in parallel with R_a the apical membrane resistance. E_a, R_a, and C_a are the apical membrane emf, resistance, and capacitance. E_{bl}, R_{bl}, and C_{bl} are the corresponding parameters for the basolateral membrane. R_j is the junctional resistance. The Na^+-specific electrode is illustrated as having a capacitance for the glass wall (C_g) and an emf and resistance for the exchanger tip (E_i and R_i). V_i is the potential measured by the high input impedance amplifier and in this case is equal to $E_i + V_{bl}$ (basolateral potential). (*B*) Shunting caused by a glass wall resistance (R_g) in parallel with the resistance of the ion exchanger at the tip (R_i) of the Na electrode. Here V_i does not equal $E_i + V_{bl}$ (for details, see text).

conductance (assuming impalement occurred across the apical membrane) to basolateral membrane conductance ($[G_D/G_{bl}]$, Lewis et al., 1978; see their Fig. 2 *b*). Such an analysis on the present data shows that all Na^+ electrodes caused significantly high G_D/G_{bl} ratios (i.e., $G_D/G_{bl} > 0$; see Fig. 3); thus this finding would at face value indicate possible impalement damage. However, two factors argue against this explanation. First, it is unlikely that all of the Na^+-specific microelectrodes caused such extensive damage, considering that both conventional and Na^+-specific microelectrodes were pulled in an identical manner. Secondly, after the microelectrode had been advanced all the way through the epithelium it still

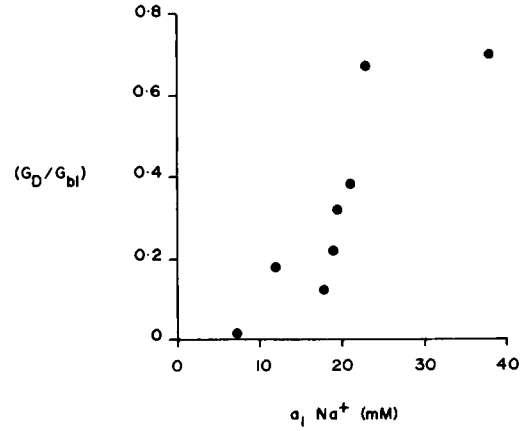

FIGURE 3 Plot of the Na^+ activity as a function of the ratio of impalement damage conductance G_D ($= {}^1/R_D$) to basolateral conductance G_{bl} ($= {}^1/R_{bl}$). See Lewis et al., 1978, p. 124 for the derivation of the ratio G_D/G_{bl}.

measured a resistance ratio. Consequently, some other feature of the Na^+-sensitive microelectrodes must account for their low resistance ratios.

Na^+-specific microelectrodes have a tip resistance (R_i) approximately one order of magnitude greater than K^+- or Cl^--specific microelectrodes (i.e., tip resistance of $\simeq 10^{10}\ \Omega$ as compared to $\simeq 10^9\ \Omega$). Eisenman (1967) and Agin (1969) have shown that the specific resistivity of glass can decrease by two to three orders of magnitude when hydrated. It is then conceivable that through hydration the resistance of the drawn glass shaft of a microelectrode can approach the resistance of the incorporated ion exchanger (see Fig. 2 *b*). Are these low α's measured with the Na^+ microelectrode caused by a glass resistance comparable to that of the tip resistance, i.e., is Fig. 2 *b* realistic?

Inspection of a current induced voltage change of the basolateral membrane measured using the Na^+-specific microelectrode (Fig. 4 *a*) indicates that there is considerable capacitative (and possibly resistive) coupling across the glass wall of the microelectrode. A conventional microelectrode fabricated in an identical manner to the Na^+ electrode with the exception that it was filled with 3 M KCl (instead of ion exchanger plus 0.5 M NaCl) neither yields low measurements of the resistance ratio nor shows the waveform (Fig. 4 *b*) of the Na^+ microelectrode.

Na^+-specific and conventional microelectrodes constructed in an identical manner produced different steady state voltage responses across the basolateral membrane to square transepithelial current pulses. Therefore, in addition to capacitative coupling across the glass there must be resistive coupling as well.

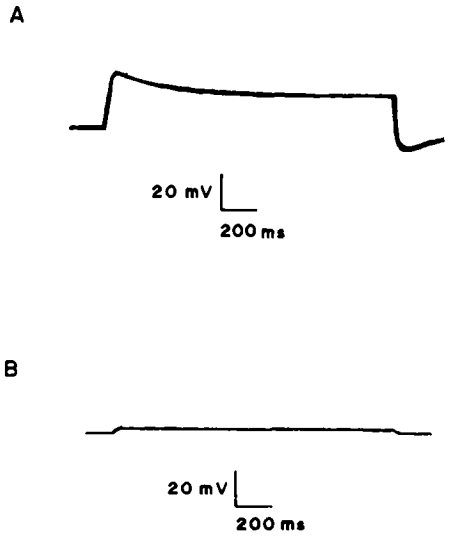

FIGURE 4 Comparison of the voltage response of the basolateral membrane to a square transepithelial current pulse measured with a sodium-specific microelectrode (*A*) and a conventional microelectrode (*B*). Note that the Na^+-specific electrode shows *RC* coupling (the initial overshoot as well as the steady state value of the voltage response to a square transepithelial current pulse), while the conventional microelectrode does not display such characteristics. In addition, the magnitude of the steady state recorded deflection by the conventional electrode is less (×10) than that measured by the Na^+ electrode indicating that even in the steady state there is a continuing current flow through the wall of the Na^+ electrode.

The ratio of the Na^+ microelectrode glass resistance (R_g) to tip resistance (R_i) can be calculated from this circuit as a comparison of the resistance ratio measured with the ion specific electrode (α_i) and conventional microelectrode (α) assuming that the apical membrane resistance (R_a) is much lower in value that the ion specific microelectrode tip resistance (R_i).[1]

$$R_g/R_i \equiv \gamma \equiv \frac{\alpha + 1}{(\alpha/\alpha_i) - 1}. \tag{1}$$

A plot of the relationship between the calculated shunting ratio (Eq. 1) and measured a_i Na^+ is shown in Fig. 5. As the ratio increases in value (less shunting) the measured a_i Na^+ decreases. The equation which describes the potential measured with a Na^+-selective microelectrode (V_i) is:

$$V_i = \frac{-E_i\gamma}{(\gamma + 1)} + \frac{Ea\left(\frac{\gamma}{\alpha} - \frac{1}{\beta}\right) - E_{bl}\left(\gamma + \frac{\gamma}{\beta} + \frac{1}{\beta}\right)}{\left(\frac{1}{\alpha} + \frac{1}{\beta} + 1\right)(\gamma + 1)}. \tag{2}$$

where $\gamma = R_g/R_i$, $\beta = R_a/R_j$, $\alpha = R_a/R_{bl}$ (see Methods for calculation), and E_i, E_a, and E_{bl} are

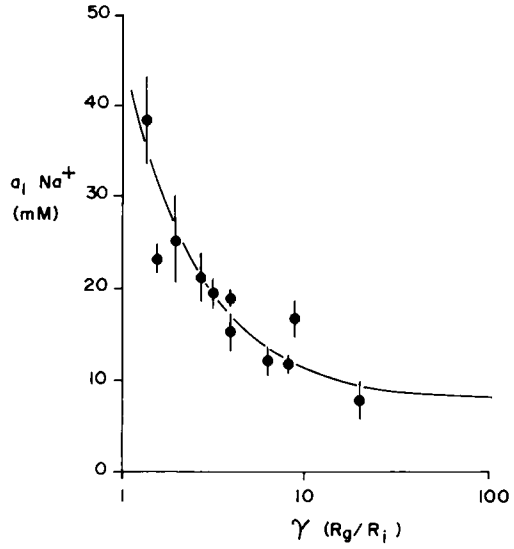

FIGURE 5 Correlation between calculated intracellular sodium activity a_i Na^+ and the ratio of glass to tip resistance of the ion specific microelectrode (γ) (see Eq. 1). Smooth curve was generated from Eq. 2 with parameters determined previously by Lewis et al. (1978) and an a_i Na^+ of 7 mM. Vertical bars are SEM.

[1]The equation which describes the ratio of glass resistance to tip resistance (R_g/R_i) without making any assumptions concerning the apical membrane and tip resistance is:

$$R_g/R_i \simeq \gamma = \frac{\alpha + 1 + (R_a/R_i)}{(\alpha/\alpha_i) - 1}.$$

the electromotive force (emf) of an electrode tip, apical and basolateral membranes, respectively. According to this equation, if one could determine the membrane emf and resistance ratios then the emf[2] (E_i) of the ion specific electrode can be calculated from the measured voltage (V_i). (See footnote 2 for assumptions in derivation).

To do this, γ (R_g/R_i) can be determined as described above, β (R_a/R_j) from estimates of apical membrane and junctional resistances using methods described by Lewis et al., (1976) and Lewis et al., (1977), and E_a and E_b by the method of Lewis et al., (1978). Performing such a calculation for each of the measurements yields a mean a_i Na^+ of 9.5 ± 2.0. The smooth curve (Fig. 5) was drawn according to equation 2, using mean calculated parameters (E_a = 16 mV, E_{bl} = 55 mV, β = 0.4, E_i = 72 mV, and α = 26).

Elimination of the Artifact

It is unlikely that impalement damage can explain all of the variation in measured a_i Na^+. However, this does not mean that the glass shunting hypothesis is correct. There are a number of methods available to test the shunting hypothesis. The most direct is to eliminate the shunt. This can be done by using (*a*) a thicker walled glass, (*b*) glass of higher resistivity, or (*c*) larger tip diameters. Some of these methods can have certain undesirable side effects. For instance, increasing tip diameter can increase the probability of impalement damage. Similarly, increased wall thickness might decrease the area of exposed ion exchange resin resulting in a microelectrode with poor temporal resolution. Rather than using a higher resistivity glass (and having to solve the problems of microelectrode fabrication and silanization), we made the glass appear to have a high resistance using an electrical method. The microelectrode was coated with a conductive silver paint to within 50 μm of the tip (electrodag 416). This layer of conductive paint was then insulated from the bathing solution first with a layer of nail hardener (Cutex) followed by M-coat D (Micro-measurements, Raleigh, N. C.) such that the resistance of the insulation was 10^{10} Ω). The conductive paint was then attached to a driven guard of the input amplifier. The net effect of this procedure was to cause the inside and outside of the microelectrode (at least to within 50 μm of the tip) to be isopotential. Thus any current loops between the tip of the microelectrode and glass wall were eliminated.

Fig. 6 *a* is an oscilloscope tracing of an impalement with the shielded Na^+-specific microelectrode. The electrical response of the microelectrode is quite rapid (note initial depolarization reflecting the basolateral membrane potential) and allows a separation between the response of the microelectrode to the membrane potential and the response of the exchanger to the intracellular Na^+ level. The measured change in basolateral membrane potential to a square transepithelial current pulse (Fig. 6 *b*) is in excellent agreement with that measured with conventional microelectrodes. In addition, the capacitive transient is now missing, indicating that the *RC* (resistive-capacitive) coupling has been virtually eliminated by the shielding procedure.

Intracellular Na^+ activities, measured with shielded microelectrodes, were 6.8 ± 1 mM. Fig. 7 indicates a normal distribution for a_i Na^+ estimated from potentials measured with

[2]Eq. 2 was derived from the equivalent circuit shown in Fig. 2 *b* for the steady state case. The simplified form of the equation is based on the assumption that the basolateral membrane and junctional resistances (R_{bl} and R_j, respectively) are small compared to the resistance of the ion exchanger (R_i). This assumption is valid even if the epithelial cells were not radially coupled, i.e., maximizing the value of R_{bl}.

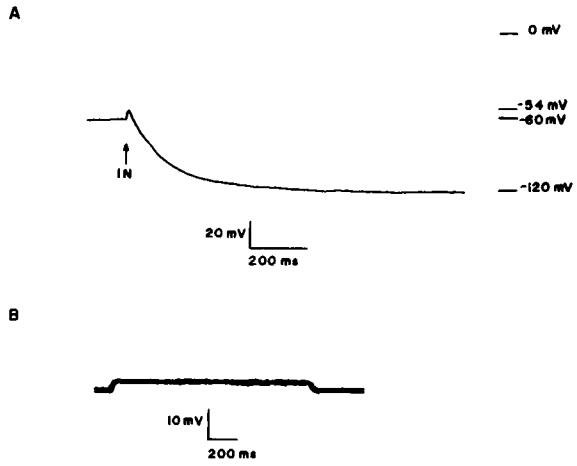

FIGURE 6 (*A*) Oscilloscope tracing (left to right) of an impalement with a shielded sodium-specific microelectrode. The baseline potential of the Na^+-specific microelectrode was adjusted to equal the transepithelial potential which was (in this tracing) −60 mV (referenced to the serosal solution). At "in" the microelectrode was advanced into the cell from the mucosal solution. The voltage response of the microelectrode is biphasic. First, there is a rapid depolarization, the peak value of this depolarization is equal to the previously measured basolateral membrane potential (this preparation had a "stairstep" potential profile). Second, there is a slower hyperpolarization which presumably is in response to the cellular Na^+ activity. (*B*) Voltage response of the basolateral membrane to a square transepithelial current pulse measured with a shielded sodium-specific microelectrode. Compared with *A*, *B* shows that shielding eliminates the *RC* coupling found with normal (unshielded) sodium-specific microelectrodes.

shielded microelectrodes. Paired measurements performed on the same tissues indicated a significantly lower estimated a_i Na^+ with shielded vs. unshielded microelectrodes or shielded microelectrodes with the driven guard disconnected ($p < 0.005$). However, after using Eq. 2 to correct for the attenuation in the unshielded or shield disconnected microelectrodes the estimated a_i Na^+ was not significantly different from that estimated from the shielded electrodes.

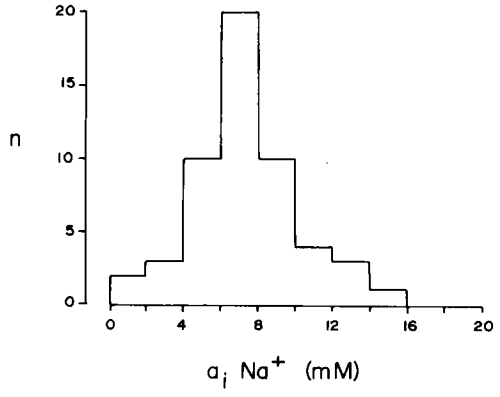

FIGURE 7 Histogram of intracellular sodium activity a_i Na^+ measurements determined from shielded sodium-specific microelectrodes. In comparison to Fig. 1, note more normal distribution and lower median Na^+ activity.

We conclude that the high and variable estimate of a_i Na^+ (Fig. 1) is largely a consequence of a shunt through the glass wall of the microelectrode and not a phenomenon of impalement damage.

DISCUSSION

In this section we discuss, in turn, some characteristics of the shunt in the microelectrode, the implications of the shunting artifact on the interpretation of estimated Na^+ activities, and the possible advantages and applications of the shielding method.

Characteristics of Microelectrode Shunt

RESISTANCE Using Eq. (1) we estimate the mean γ ($\equiv R_g/R_i$) as 4. The electrical resistance of a shielded Na^+ microelectrode is $\simeq 2 \times 10^{10}$ Ω when bathed in 100 mM NaCl. Knowing the values for R_i and γ, the shunt resistance is $\simeq 8 \times 10^{10}$ Ω.

CAPACITANCE From the basolateral membrane voltage response (measured using an unshielded Na^+ microelectrode) to a square transepithelial current pulse, the shunt capacitance can be estimated, and is $\sim 20 \times 10^{-12}$ F. Given the resistance and capacitance of the unshielded microelectrode, it would take $\simeq$2.0 s to reach 99.9% of the final microelectrode potential after impaling the cells (assuming the response to the exchanger is instantaneous).

LOCALIZATION Two general pathways for the shunt are either directly through the glass, as indicated by Fig. 2 *b*, or alternately along the outside glass surface, to the open end of the microelectrode barrel. The latter possibility is unlikely for the following reasons. First, the microelectrode resistance is independent of the depth of solution covering the electrode (minimum depth of 0.5 mm). Second, a silicon grease seal placed around the shaft, between the tip and the open end of the microelectrode, does not alter the resistance properties.

SELECTIVITY Comparison of the slopes and selectivities (Table I) of unshielded and shielded Na^+-selective microelectrodes will yield some qualitative information concerning the selectivity of this shunt pathway. Three cases are considered. First, if the shunt is non-selective, the slope of the microelectrode will decrease 20% (since the ratio of shunt to tip

TABLE I
COMPARISON OF SHIELDED AND UNSHIELDED Na^+-SENSITIVE MICROELECTRODE CHARACTERISTICS

	Na^+:K^+ selectivity	Slope (mV/decade change in Na^+ activity)
Unshielded $N = 11$	14:1	57 ± 2
Shielded $N = 8$	26:1	60 ± 1

Na^+ activity equation:

$$a_i Na^+ = [a_0 Na^+ + K_{K/Na} \cdot a_0 K^+] \left[\exp \frac{nF}{RT}(V_{Na} - V_{bl})\right] - K_{K/Na} a_i K^+,$$

where $K_{K/Na}$ is the sensitivity to competing ions, V_{Na} is the Na^+-sensitive microelectrode reading, a_i and a_0 refer to intracellular or outside bathing solution activity, and n, F, R, and T have their usual meaning.

resistance is 4:1). Second, if the shunt is anion selective, the percent decrease in slope will be greater and selectivity will be poor. Last, if the shunt is cation selective, the slope will decrease only slightly and, depending on the P_{Na}/P_K selectivity of the shunt, the microelectrode selectivity might remain unchanged or decrease. The data in Table I indicates that the shunt is cation selective.

Knowing the volume resistivity of the glass (10^{15} Ωcm at 25°C) and the shape of the electrode, we can estimate the resistance of the glass portion of the microelectrode. Considering the shape as a right cone of height 1.5 cm, base radius 0.05 cm, and a constant ratio of wall thickness to radius, the estimated resistance is 3×10^{13} Ω, two and a half orders of magnitude greater than what we measured. This discrepancy between measured and calculated glass resistance can be explained by the findings of Eisenman (1967) and Agin (1969) in which hydrated glass can have a resistance some two to three orders of magnitude less than unhydrated glass.

The glass resistance of the unshielded tip (50 μm) is 5×10^{13} Ω, yielding a $\gamma \simeq 2{,}500$ on the assumption that the hydrated glass resistivity is two orders of magnitude less than unhydrated glass resistivity. This large value for γ would cause an ~0.02% overestimate of a_i Na^+.

In summary of this section, although a microelectrode might demonstrate a nearly ideal slope and reasonable selectivity, the resistance and selectivity properties of the microelectrode may not necessarily be confined to the tip. Shielding the microelectrode eliminated (within measuring accuracy) this shunting artifact. Furthermore, it would appear that the shunt is through the glass wall rather than a surface-conductive pathway.

Consequences of Shunting Artifact

As already shown, the shunting artifact can cause a considerable overestimate of the calculated a_i Na^+. The effect of the shunt on the measured potential (V_i) is shown by Eq. 2. V_i is the sum of two potentials, the intracellular ion activity signal with respect to the bathing solution and the membrane potential. The shunt in the electrode attenuates both of these electrical signals. Both activity and membrane potential signals vary as a function of the ratio of glass to tip resistance. In addition, the amount of attenuation of the membrane potential signal is dependent on the epithelium resistances and emf. As an example, in the rabbit urinary bladder, as Na^+ transport (from urine to plasma) increases, the following parameters change: E_a increases (the apical membrane emf approaches the value of the Nernst potential for Na^+), α (apical to basolateral resistance ratio), and β (apical to junctional resistance ratio) decreases, i.e., the apical membrane becomes more permeable to Na^+. The net result of these changes is that as the rate of Na^+ transport increases, the estimated a_i Na^+ (for an unshielded microelectrode) decreases. If we were unaware of the shunting artifact, the apparent decrease of a_i Na^+ (as transport increases) would result in incorrect conclusions about the regulation and rate limiting steps of net Na^+ transport.

Does this shunting problem exist for the K^+- or Cl^--specific microelectrodes? The answer is probably yes, at least for the K^+-specific microelectrode. However, the magnitude of the shunting effect will be decreased because the resistance of the K^+-specific microelectrode is approximately one order of magnitude less ($\simeq 2 \times 10^9$ Ω) than the Na^+-specific microelectrode ($\simeq 2 \times 10^{10}$ Ω) (given the same micropipette geometry). Could the "damage" reported by Lewis et al. (1978) be a consequence of such shunting? Fig. 8 is a plot of their data, expressed

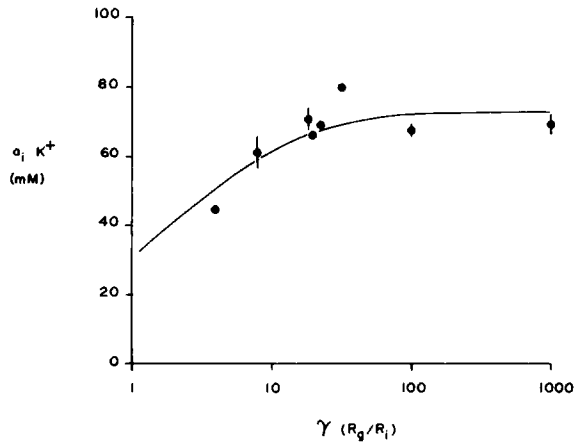

FIGURE 8 A plot of a_i K^+ vs. γ. Data from Lewis et al. (1978). Smooth curve derived from Eq. (2). Parameters used to generate this curve are given in the text.

as a function of γ. The smooth curve was drawn according to Eq. 2 where $E_i = -68$ mV and remaining membrane parameters were as given in Results. The predicted effect of a shunt on calculated a_i K^+ is in agreement with the measured values. Consequently, K^+ electrodes are also susceptible to shunting, although to a lesser degree.

Applications and Advantages

The most obvious advantage of shielding the microelectrode is the elimination of the glass as a possible source of a shunt pathway which could result in incorrect estimates of intracellular ion activities. An added bonus of such shielding is an increase in the frequency response of the microelectrode. It is obvious that a shunt acting as a parallel resistor capacitor network through the glass of the microelectrode will cause a decrease in the response either to applied voltage stimuli or upon impalement of the preparation. The rate of response of the microelectrode will be a function of the time constant of the glass. Reduction of this time constant allows a more accurate monitoring of time varying potentials.

A disadvantage of this system is that after removal of the glass capacitor, a high frequency filter has been eliminated. Thus, shielded microelectrodes have more high frequency noise contamination, which can, however, be reduced by using a low pass filter (e.g., the filter used on many oscilloscope differential amplifier inputs or paper chart recorders).

Other than increasing the frequency response of the electrodes, the elimination of capacitative coupling across the wall of the glass reduces noise pickup from such sources as magnetic stirrers and aeration systems. Thus, in our system we are able to maintain both stirring and bubbling of the bathing solutions with a minimum of interference.

The method of shielding electrodes has been used by excitable membrane physiologists for a number of years to eliminate capacitative coupling between bathing solution and current passing microelectrodes. Recently Suzuki et al. (1978) described two shielding systems for the reduction of capacitative coupling between current passing bathing solution electrodes and voltage measuring microelectrodes. In this report we use one of these shielding methods but for the intent of eliminating not only capacitative coupling but also resistive coupling.

We wish to thank Doctors B. Biagi, C. Cohen, E. Marban, R. C. Thomas, and R. W. Tsien for careful and critical review of this manuscript.

This work was supported by National Institutes of Health grant AM 20851. Dr. Wills was a National Institutes of Health Postdoctoral Fellow.

Received for publication 20 November 1979 and in revised form 27 February 1980.

REFERENCES

1. AGIN, D. P. 1969. Electrochemical properties of glass microelectrodes. *In* Glass Microelectrodes. M. Lavallee, O. F. Schanne, and N. C. Herbert, editors. Wiley and Sons, Inc. Toronto. 62.
2. EATON, D. C., J. M. RUSSELL, and A. M. BROWN. 1975. Ionic permeabilities of an *Aplysia* giant neuron. *J. Membr. Biol.* **21**:353.
3. EISENMAN, G. 1967. The origin of the glass electrode potential. *In* Glass Electrodes for Hydrogen and Other Cations. G. Eisenman, editor. Marcel Dekker Inc. New York. 133.
4. LEWIS, S. A. 1977. A reinvestigation of the function of the mammalian urinary bladder. *Am. J. Physiol.* **232**:F187.
5. LEWIS, S. A., and J. M. DIAMOND. 1976. Na^+ transport by rabbit urinary bladder, a tight epithelium. *J. Membr. Biol.* **28**:1.
6. LEWIS, S. A., D. C. EATON, C. CLAUSEN, and J. M. DIAMOND. 1977. Nystatin as a probe for investigating the electrical properties of a tight epithelium. *J. Gen. Physiol.* **70**:427.
7. LEWIS, S. A., N. K. WILLS, and D. C. EATON. 1978. Basolateral membrane potential of a tight epithelium: ionic diffusion and electrogenic pumps. *J. Membr. Biol.* **41**:117.
8. O'DOHERTY, J., J. F. GARCIA-DIAZ, and W. M. ARMSTRONG. 1979. Sodium-selective liquid ion-exchanger microelectrodes for intracellular measurements. *Science (Wash. D.C.)* **203**:1349.
9. SUZUKI, K., V. ROHLICEK, and E. FRÖMTER. 1978. A quasi-totally shielded, low-capacitance glass-microelectrode with suitable amplifiers for high-frequency intracellular potential and impedence measurements. *Pflügers Archiv.* **378**:141.
10. STEINER, R. A., M. OEHME, D. AMMANN, and W. SIMON. 1979. Neutral carrier sodium ion-selective microelectrode for intracellular studies. *Anal. Chem.* **51**:351.